NATIONAL ADVISORY COMMITTEE FOR AERONAUTICS

TECHNICAL NOTE 4174

WIND-TUNNEL INVESTIGATION OF THE STATIC LATERAL

STABILITY CHARACTERISTICS OF WING-FUSELAGE

COMBINATIONS AT HIGH SUBSONIC SPEEDS

TAPER-RATIO SERIES

By James W. Wiggins and Paul G. Fournier

Langley Aeronautical Laboratory
Langley Field, Va.

NACA

Washington

October 1957

NATIONAL ADVISORY COMMITTEE FOR AERONAUTICS

TECHNICAL NOTE 4174

WIND-TUNNEL INVESTIGATION OF THE STATIC LATERAL

STABILITY CHARACTERISTICS OF WING-FUSELAGE

COMBINATIONS AT HIGH SUBSONIC SPEEDS

TAPER-RATIO SERIES[1]

By James W. Wiggins and Paul G. Fournier

SUMMARY

An investigation was conducted in the Langley high-speed 7- by 10-foot tunnel to determine the effects of variations in taper ratio within the range of 0.3 to 1.0 on the static lateral stability characteristics at high subsonic speeds of wing-fuselage combinations having wings of 45° sweepback at the quarter-chord line and an aspect ratio of 4. As has been shown in previous experimental investigations of other wing plan forms, the parameter C_{l_β}/C_L, which expresses the rate of change of effective dihedral with lift coefficient, was found to increase at the high subsonic Mach numbers as the force-break Mach number was approached. Above the force-break Mach number, C_{l_β}/C_L decreased in magnitude with the severity of the break increasing with a decrease in taper ratio. The experimental variation of C_{l_β}/C_L increases negatively with taper ratio and agrees well with the predicted trend; however, the experimental values are shown to be appreciably larger than the predicted values. At low and moderate lift coefficients the derivative of yawing moment due to sideslip C_{n_β} and lateral force due to sideslip C_{Y_β} for the wing-fuselage combinations are contributed almost entirely by the fuselage alone; however, at high lift coefficients the effects of the wing are quite large.

INTRODUCTION

A systematic research program is being carried out in the Langley high-speed 7- by 10-foot tunnel to determine the aerodynamic characteristics of various arrangements of the component parts of research-type

airplane models, including some complete model configurations. Data are being obtained on characteristics in pitch, sideslip, and during steady roll at Mach numbers from 0.40 to about 0.95.

This paper presents results which show the effect of taper ratio on the aerodynamic characteristics in sideslip of wing-fuselage combinations having wings with a sweep of 45° at the quarter-chord line, an aspect ratio of 4, and an NACA 65A006 airfoil section. The three wings have taper ratios of 0.3, 0.6, and 1.0. Investigations of the effects of sweep and aspect ratio on lateral stability characteristics are presented in references 1 and 2, respectively. The characteristics of the fuselage alone, which has been common to all configurations covered in the program, are included in reference 1. In order to expedite the issuance of the results, only a limited comparison of some of the more significant characteristics with available theory is presented in this paper.

COEFFICIENTS AND SYMBOLS

The stability system of axes used for the presentation of the data, together with an indication of the positive forces, moments, and angles, is presented in figure 1. All moments are referred to the quarter-chord point of the mean aerodynamic chord.

C_L lift coefficient, $\dfrac{\text{Lift}}{qS}$

C_l rolling-moment coefficient, $\dfrac{\text{Rolling moment}}{qSb}$

C_n yawing-moment coefficient, $\dfrac{\text{Yawing moment}}{qSb}$

C_Y lateral-force coefficient, $\dfrac{\text{Lateral force}}{qS}$

q dynamic pressure, $\dfrac{\rho V^2}{2}$, lb/sq ft

ρ mass density of air, slugs/cu ft

V free-stream velocity, fps

M   Mach number

R   Reynolds number, $\dfrac{\rho V \bar{c}}{\mu}$

μ absolute viscosity of air, slugs/ft-sec

S   wing area, sq ft

b   wing span, ft

c   wing chord, ft

$\bar{c}$ mean aerodynamic chord, $\dfrac{2}{S} \displaystyle\int_0^{b/2} c^2 dy$, ft

y   spanwise distance from plane of symmetry, ft

α angle of attack, deg

β angle of sideslip, deg

δ deflection, ft

$C_{l_\beta} = \dfrac{\partial C_l}{\partial \beta}$ per deg

$C_{n_\beta} = \dfrac{\partial C_n}{\partial \beta}$ per deg

$C_{Y_\beta} = \dfrac{\partial C_Y}{\partial \beta}$ per deg

$\dfrac{C_{l_\beta}}{C_L} = \dfrac{\partial C_{l_\beta}}{\partial C_L}$ per deg

Subscript:

WF-F   wing-fuselage values minus fuselage values

MODEL AND APPARATUS

The wing-fuselage combinations tested are shown in figure 2. All
wings had an NACA 65A006 airfoil section parallel to the plane of sym-
metry and were attached to the fuselage in a midwing position. All
wings were constructed of solid aluminum alloy except the taper-ratio-0.6
wing which was of composite construction, consisting of a steel core and
a bismuth-tin covering. The aluminum fuselage was common to all configu-
rations and its ordinates are presented in reference 3.

The three wings used in this investigation represent only a part
of a family of wings being studied in a more extensive program; there-
fore, a common wing designation system is being used for the entire
program. For example, the wing designated by 45-4-0.6-006 has the
quarter-chord line swept back 45°, an aspect ratio of 4, and a taper
ratio of 0.6. The number 006 refers to the section designation; in
this case the design lift coefficient is zero and the thickness is
6 percent of the chord.

The models were tested on the sting support system shown in fig-
ures 3 and 4. With this support system the model can be remotely
operated through a 28° angle range in the plane of the vertical strut.
By means of couplings in the sting, the model can be rolled through 90°
so that either angle of attack (fig. 3) or angle of sideslip (fig. 4)
can be the remotely controlled variable. With the model horizontal
(fig. 3) couplings can be used to support the model at angles of side-
slip of approximately -4° or 4° while the model is tested through the
angle-of-attack range.

TEST AND CORRECTIONS

The tests were conducted in the Langley high-speed 7- by 10-foot
tunnel through a Mach number range from 0.40 to 0.95. The size of the
models caused the tunnel to choke at corrected Mach numbers of 0.95
to 0.96, depending on the wing being tested. The blocking corrections
which were applied to the data were determined by the velocity-ratio
method of reference 4.

The present investigation consisted of two groups of tests. The
first, from which most of the data were obtained, involved runs at angles
of sideslip of -4° and 4° through an angle-of-attack range from -3°
to 24°. The second series of tests were made at several predetermined
angles of attack through a sideslip-angle range from 4° to -10°.

The jet-boundary corrections applied to the angle of attack were determined by the method of reference 5. The corrections to lateral force, yawing moment, and rolling moment were considered negligible. Tare corrections were obtained but were found to be negligible for a wing-fuselage configuration and therefore were not applied. The angle of attack and the angle of sideslip have been corrected for the deflection of the sting support system and balance under load.

Corrections for the spanwise dihedral distribution due to wing distortion while under aerodynamic load (figs. 5 and 6) have been applied to these data and were determined by the method discussed in detail in reference 1.

The Reynolds number variations with test Mach number are presented in figure 7 for the three wings. Reynolds numbers range from 1.75×10^6 to 3.20×10^6 and are based on the mean aerodynamic chord of the respective wing.

RESULTS AND DISCUSSION

The basic data for the wing-fuselage configurations having wings of taper ratios of 0.3 and 1.0 are presented in figures 8 and 9, respectively. The basic data for the 0.6-taper-ratio-wing—fuselage configuration and for the fuselage alone are presented in reference 1. The basic data have not been corrected for aeroelastic distortion. The bulk of the data was obtained from tests at angles of sideslip of $-4°$ and $4°$. The flagged symbols (figs. 8, 9, and ref. 1) are results obtained from tests in which the angle of sideslip was the variable.

A sample of the data obtained through the sideslip-angle range is presented in reference 1. As was pointed out in references 1 and 2, the lateral force and yawing moment are contributed almost entirely by the fuselage.

Rolling-Moment Characteristics

A comparison of the variation of the effective dihedral parameter C_{l_β} with lift coefficient for the three wing-fuselage configurations is presented in figure 10. Wing-plus-wing-fuselage-interference data (fig. 11) were obtained by subtracting the fuselage-alone data of reference 1 from the data of figure 10 and indicate essentially the same trends as the wing-fuselage data. At low lift coefficients the rate of change of C_{l_β} with lift coefficient increases negatively with an increase

in taper ratio at all Mach numbers. The lift coefficient at which the initial break in C_{l_β} occurs and the maximum value of C_{l_β} at this lift coefficient increase with an increase in taper ratio at the higher Mach numbers. This initial break in the C_{l_β} curve probably is caused by loss of lift on the forward wing panel. As a result, values of C_{l_β} become positive at lift coefficients around 0.7 or 0.8 for all wings at the lower Mach numbers; however, results from the 0.3-taper-ratio wing indicate a recovery from this condition at a lower Mach number than for the wings of taper ratio 0.6 and 1.0 (figs. 8, 9, and 10). The range of lift coefficient over which C_{l_β} is linear increases with Mach number up to the force break ($M \approx 0.93$) for the wings of taper ratios of 0.6 and 1.0 (fig. 9 and ref. 1), but the results from the 0.3-taper-ratio wing (fig. 8) indicate essentially no effect of Mach number on the linear range of C_{l_β} at these Mach numbers.

The variation of the slope C_{l_β}/C_L, measured near zero lift, with Mach number is presented in figure 12 and the variation with taper ratio is shown in figure 13 along with a comparison with wing-alone theory and experimental values corrected for aeroelastic distortion. The theoretical predictions were determined by applying the compressibility corrections calculated by the method of reference 6 to the incompressible-flow values calculated by the method of reference 7. As was generally found for the wings investigated in references 1 and 2, values of C_{l_β}/C_L increased at the higher subsonic Mach numbers as the force-break Mach number was approached for each of the wing-fuselage combinations; although the present available theory (ref. 6) predicts a slight decrease in C_{l_β}/C_L within this Mach number range.

All wing-fuselage combinations exhibited a reduction in C_{l_β}/C_L above the force-break Mach number, with the severity of the break increasing with a decrease in taper ratio.

The experimental variation of C_{l_β}/C_L with taper ratio (fig. 13) agrees well with the predicted variation; however, as also shown in figure 12, the experimental values are appreciably greater than the predicted values.

Lateral-Force and Yawing-Moment Characteristics

Comparisons of the variations of the lateral-stability parameters C_{n_β} and C_{Y_β} with lift coefficient are presented in figures 14 and 15

for the wing-fuselage configurations. The wing-plus-wing-fuselage-interference data for the same conditions, which were obtained by subtracting the fuselage-alone data of reference 1 from the data of figures 14 and 15 are presented in figures 16 and 17.

The results indicate that, at lift coefficients below about 0.8, the derivatives C_{n_β} and C_{Y_β} are contributed almost entirely by the fuselage alone. The breaks in the curves at the higher lift coefficients are probably due to wing stalling which changes the magnitude and orientation of the resultant force on the two wing semispans.

CONCLUSIONS

The results of the present investigation of the aerodynamic characteristics in sideslip at high subsonic speeds of wings having various taper ratios, with a sweep angle of 45°, an aspect ratio 6, and an NACA 65A006 airfoil section indicate the following conclusions:

1. The experimental variation of C_{l_β}/C_L (rate of change of effective dihedral with lift coefficient) indicates an increase in magnitude at the higher subsonic Mach numbers up to the force break. This trend is in general agreement with experimental results obtained in other investigations, although available theory indicates that a slight decrease in this derivative with increasing Mach number should be expected. Above the force-break Mach number the parameter C_{l_β}/C_L exhibited a reduction with a further increase in Mach number, with the severity of the break increasing with a decrease in taper ratio.

2. The experimental variation of C_{l_β}/C_L increases negatively with taper ratio and agrees well with the predicted trend; however, the experimental values are shown to be appreciably greater than the predicted values.

3. At low and moderate lift coefficients the derivative of yawing moment due to sideslip C_{n_β} and lateral force due to sideslip C_{Y_β} for the wing-fuselage combinations are contributed almost entirely by the fuselage alone; however, at high lift coefficients the effects of the wing are quite large.

Langley Aeronautical Laboratory,
    National Advisory Committee for Aeronautics,
        Langley Field, Va., February 25, 1953.

REFERENCES

1. Kuhn, Richard E., and Fournier, Paul G.: Wind-Tunnel Investigation
   of the Static Lateral Stability Characteristics of Wing-Fuselage
   Combinations at High Subsonic Speeds - Sweep Series. NACA
   RM L52G11a, 1952.

2. Fournier, Paul G., and Byrnes, Andrew L., Jr.: Wing-Tunnel Investiga-
   tion of the Static Lateral Stability Characteristics of Wing-
   Fuselage Combinations at High Subsonic Speeds - Aspect-Ratio Series.
   NACA RM L52L18, 1953.

3. Kuhn, Richard E., and Wiggins, James W.: Wind-Tunnel Investigation
   of the Aerodynamic Characteristics in Pitch of Wing-Fuselage Com-
   binations at High Subsonic Speeds - Aspect-Ratio Series. NACA
   RM L52A29, 1952.

4. Hensel, Rudolpf W.: Rectangular-Wind-Tunnel Blocking Corrections
   Using the Velocity-Ratio Method. NACA TN 2372, 1951.

5. Gillis, Clarence L., Polhamus, Edward C., and Gray, Joseph L., Jr.:
   Charts for Determining Jet-Boundary Corrections for Complete Models
   in 7- by 10-Foot Closed Rectangular Wind Tunnels. NACA WR L-123,
   1945. (Formerly NACA ARR L5G31.)

6. Fisher, Lewis R.: Approximate Corrections for the Effects of Com-
   pressibility on the Subsonic Stability Derivatives of Swept Wings.
   NACA TN 1854, 1949.

7. Toll, Thomas A., and Queijo, M. J.: Approximate Relations and Charts
   for Low-Speed Stability Derivatives of Swept Wings. NACA TN 1581,
   1948.
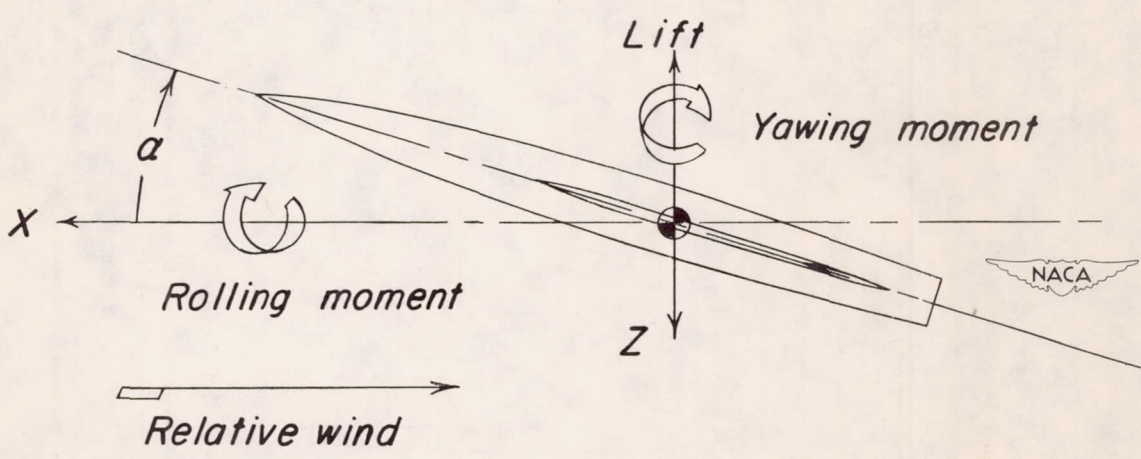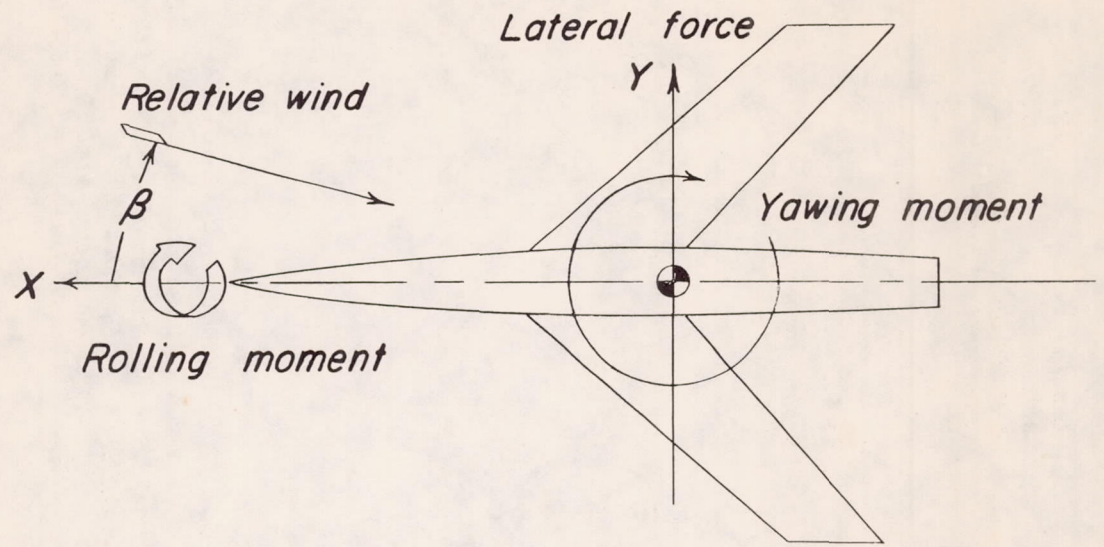
Figure 1.- System of axes used showing the positive direction of forces, moments, and angles.

Wing geometry

Area	2.25 sq ft
Span	3.00 ft
Sweep at 0.25 chord line	45°
Aspect ratio	4
Incidence	0
Dihedral	0
Airfoil section parallel to fuselage $\mathcal{C}$	NACA 65 A006

Fuselage

Length	49.20 in.
Max. diam.	5.00 in.
Position of max. diam.	30.00 in.
(from nose of model)	

Scale , inches
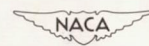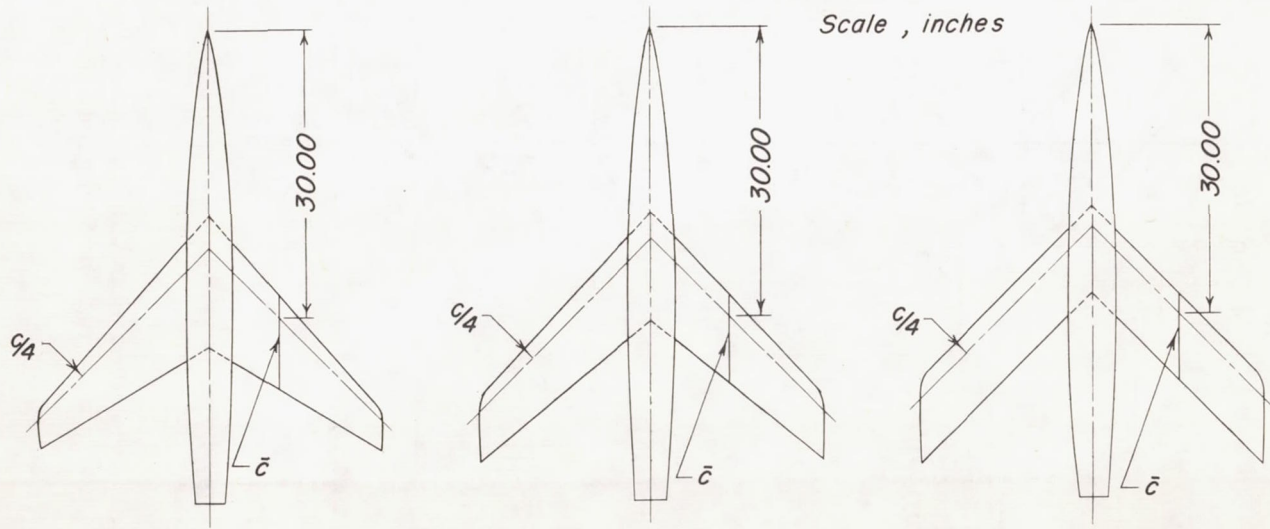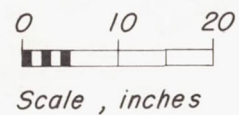
Wing   45 - 4 - 0.3 - 006

Taper ratio	0.3
Root chord	13.85 in.
Tip chord	4.16 in.
Mean aerodynamic chord	0.822 ft

Wing   45 - 4 - 0.6 - 006

Taper ratio	0.6
Root chord	11.25 in.
Tip chord	6.75 in.
Mean aerodynamic chord	0.765 ft

Wing   45 - 4 - 1.0 - 006

Taper ratio	1.0
Root chord	9.00 in.
Tip chord	9.00 in.
Mean aerodynamic chord	0.750 ft

Figure 2.- Drawing of the three wing-fuselage configurations.
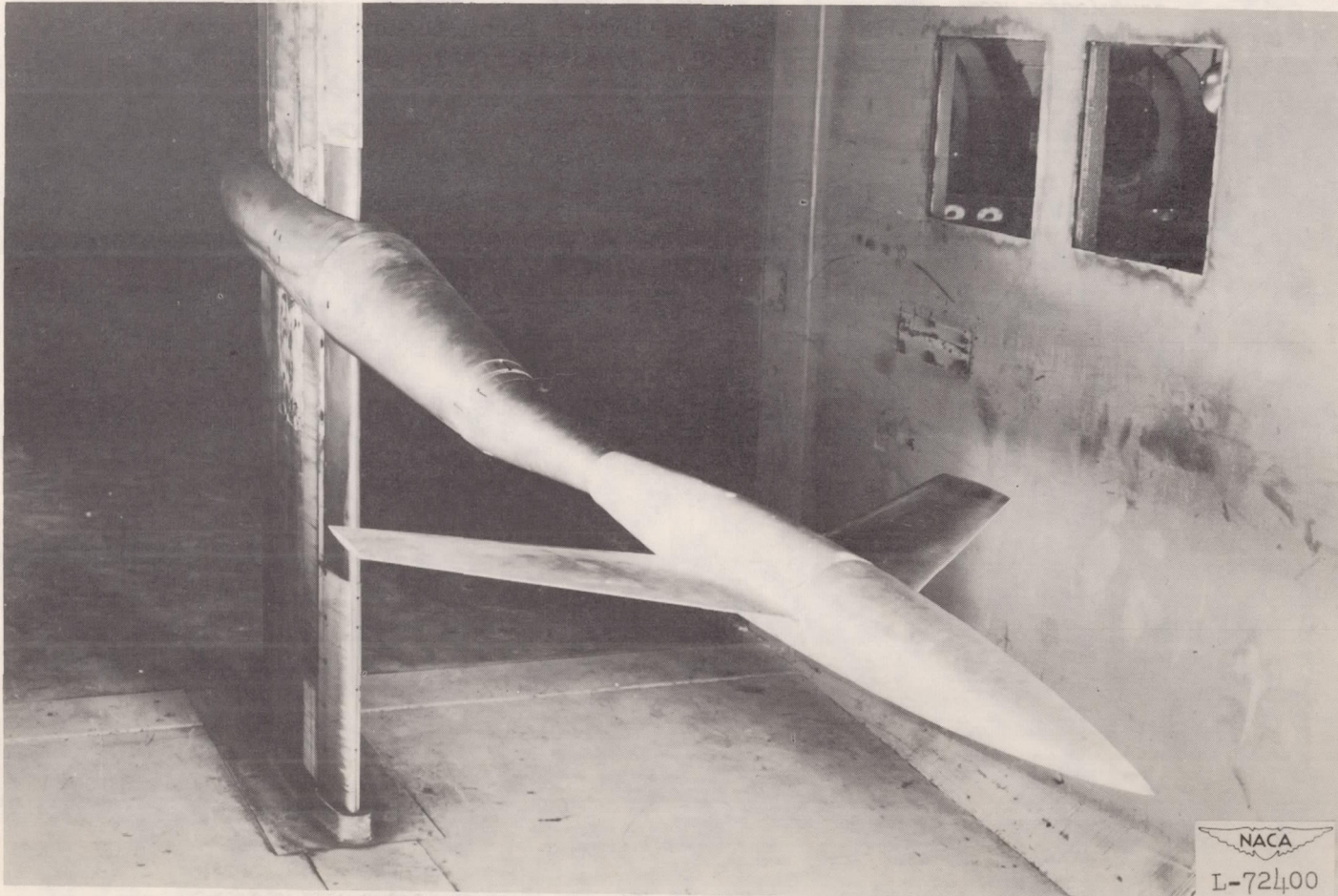
Figure 3.- A typical model installed on the sting support system for variable angle-of-attack tests. Shown at 4° angle of sideslip.
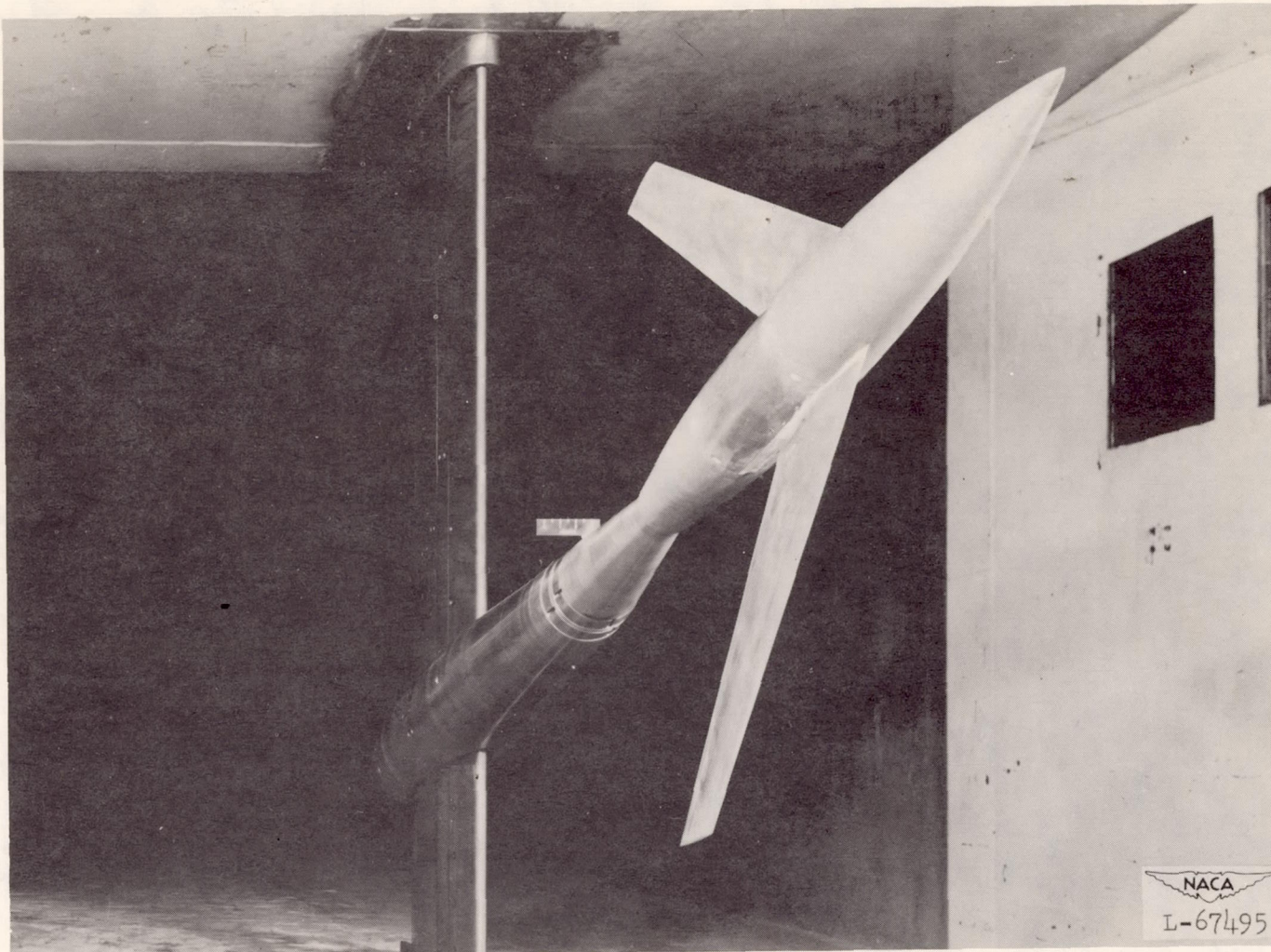
Figure 4.- A typical model installed for variable angle-of-sideslip tests. Shown at 0° angle of attack.

$$\frac{\delta/\frac{b}{2}}{qC_L}$$

.00010

.00005

0

45-4-1.0-006

45-4-.6-006

45-4-.3-006

0   .2   .4   .6   .8   1.0

$y/b/2$
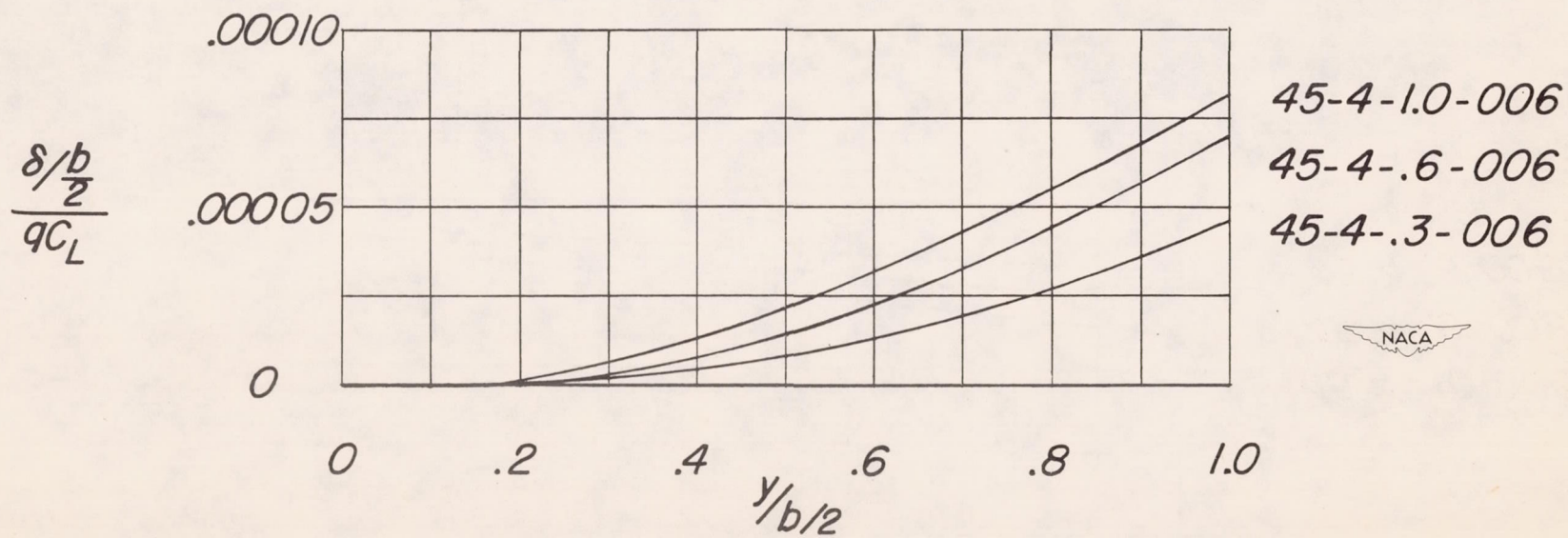
Figure 5.- Deflection curves for the test wings.
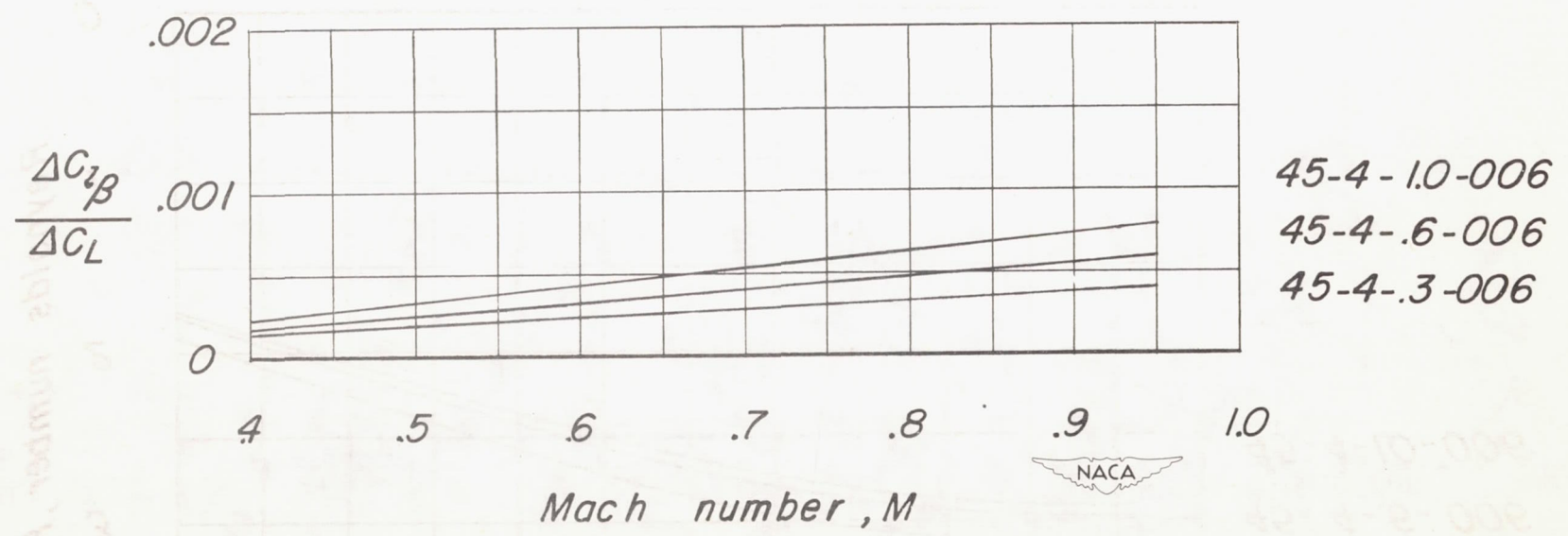
Figure 6.- Correction factors used to correct for the effects of aero-
elastic distortion.
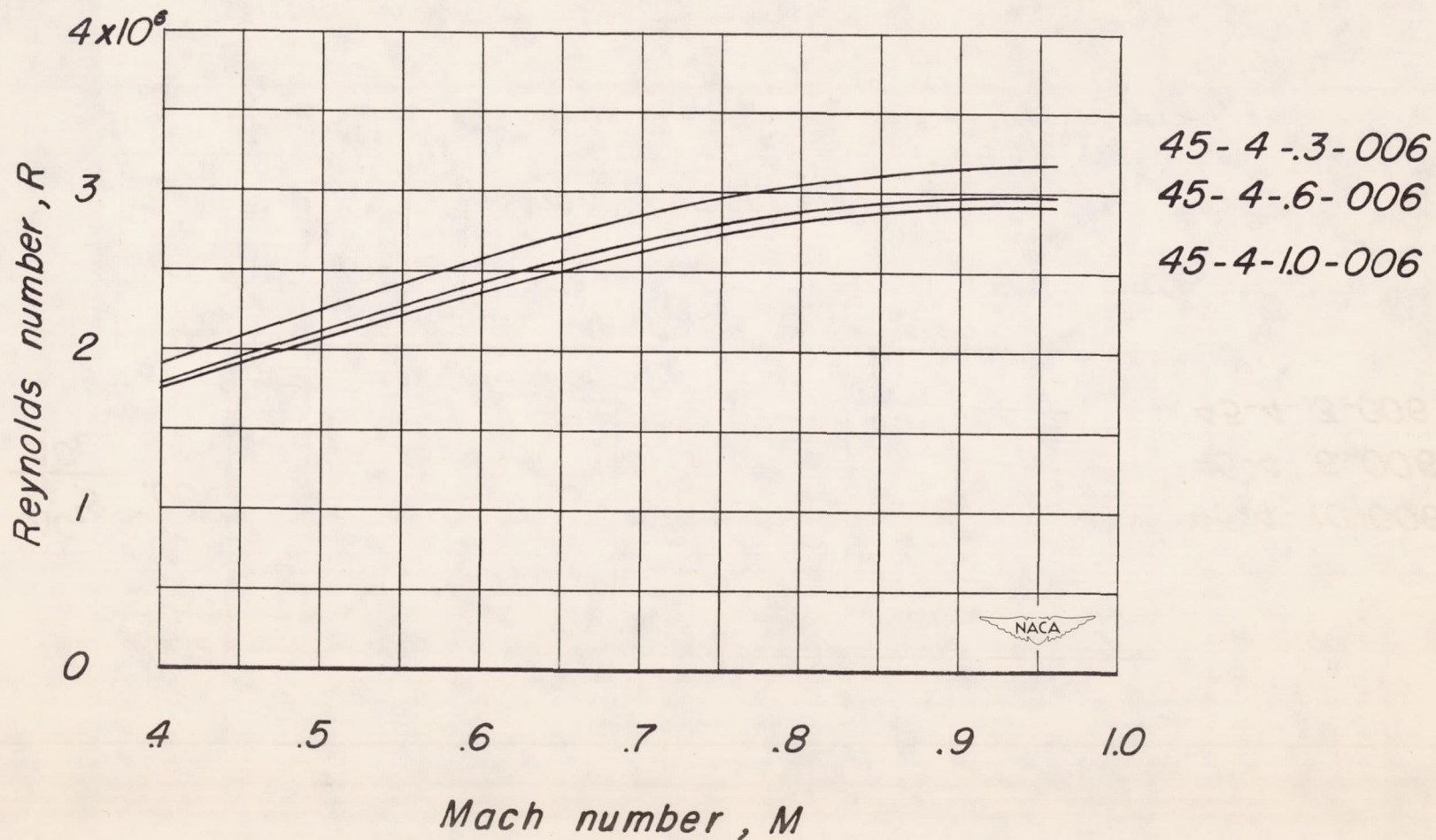
Figure 7.- Variation of mean Reynolds number with test Mach number based on the wing mean aerodynamic chord.
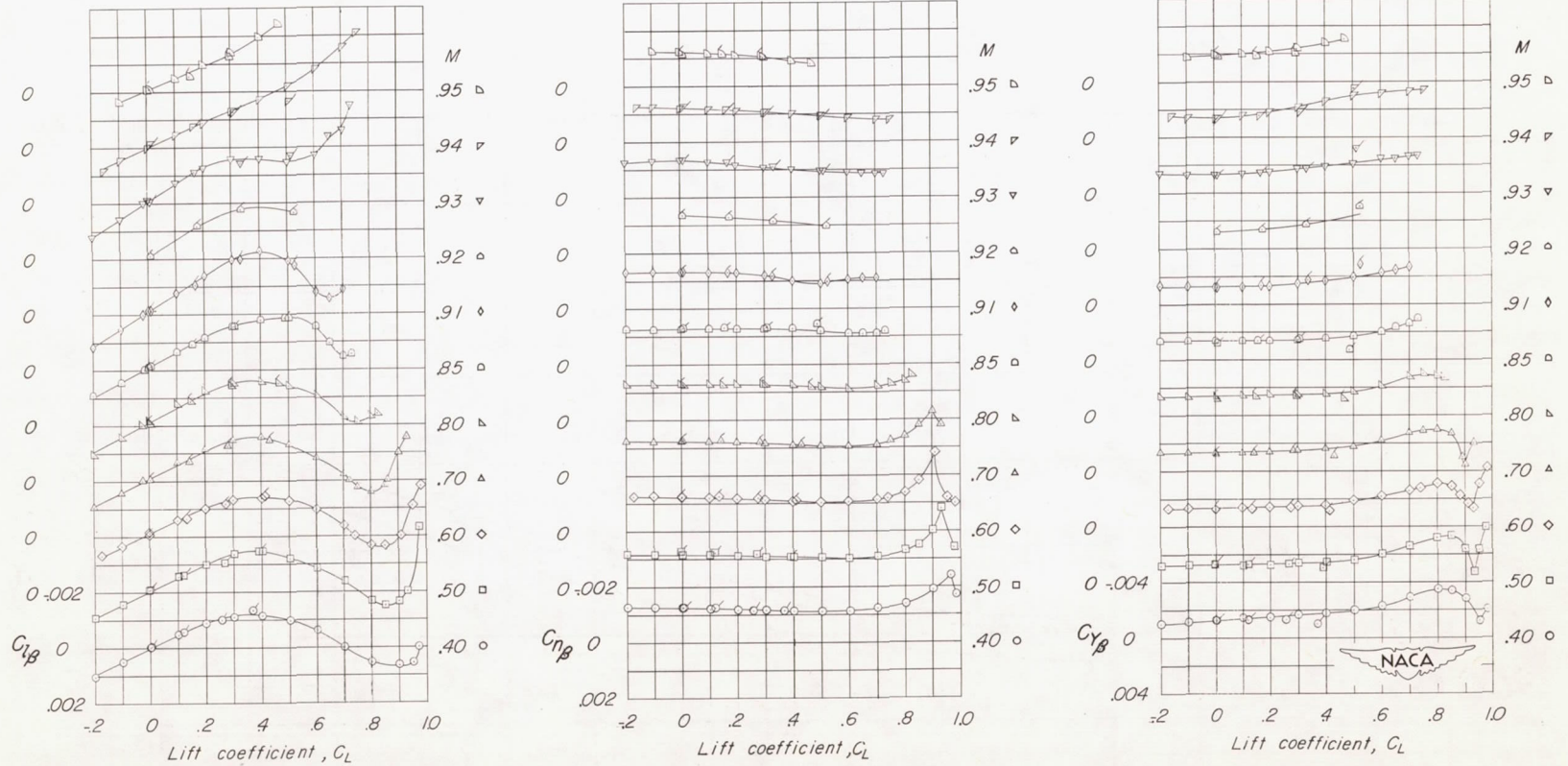
Figure 8.- Lateral stability characteristics of the 45-4-0.3-006 wing-
fuselage combination. Not corrected for aeroelastic distortion.
Flagged symbols represent tests in which the angle of sideslip was
varied.
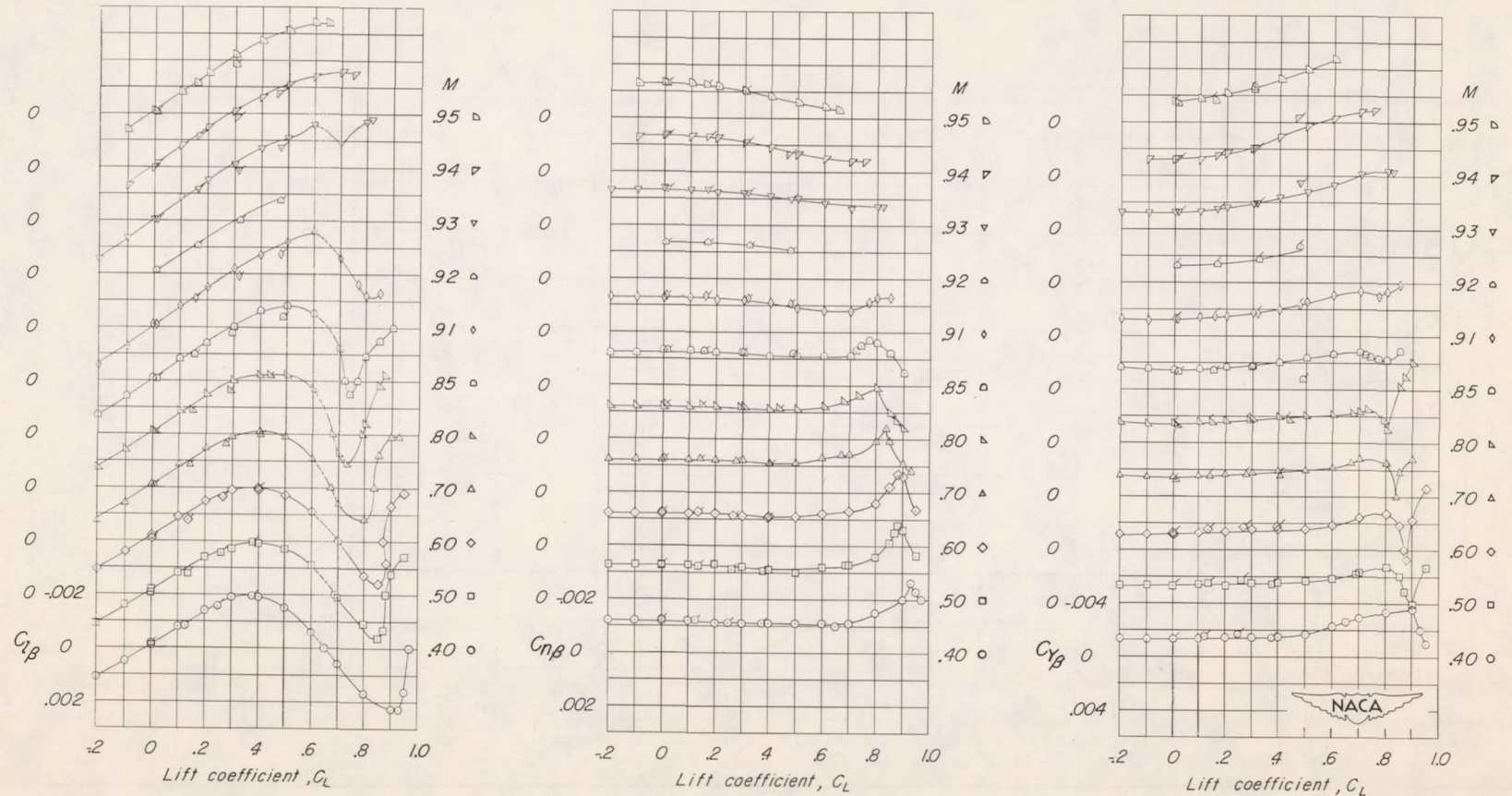
Figure 9.- Lateral stability characteristics of the 45-4-1.0-006 wing-fuselage combination. Not corrected for aeroelastic distortion. Flagged symbols represent tests in which the angle of sideslip was varied.
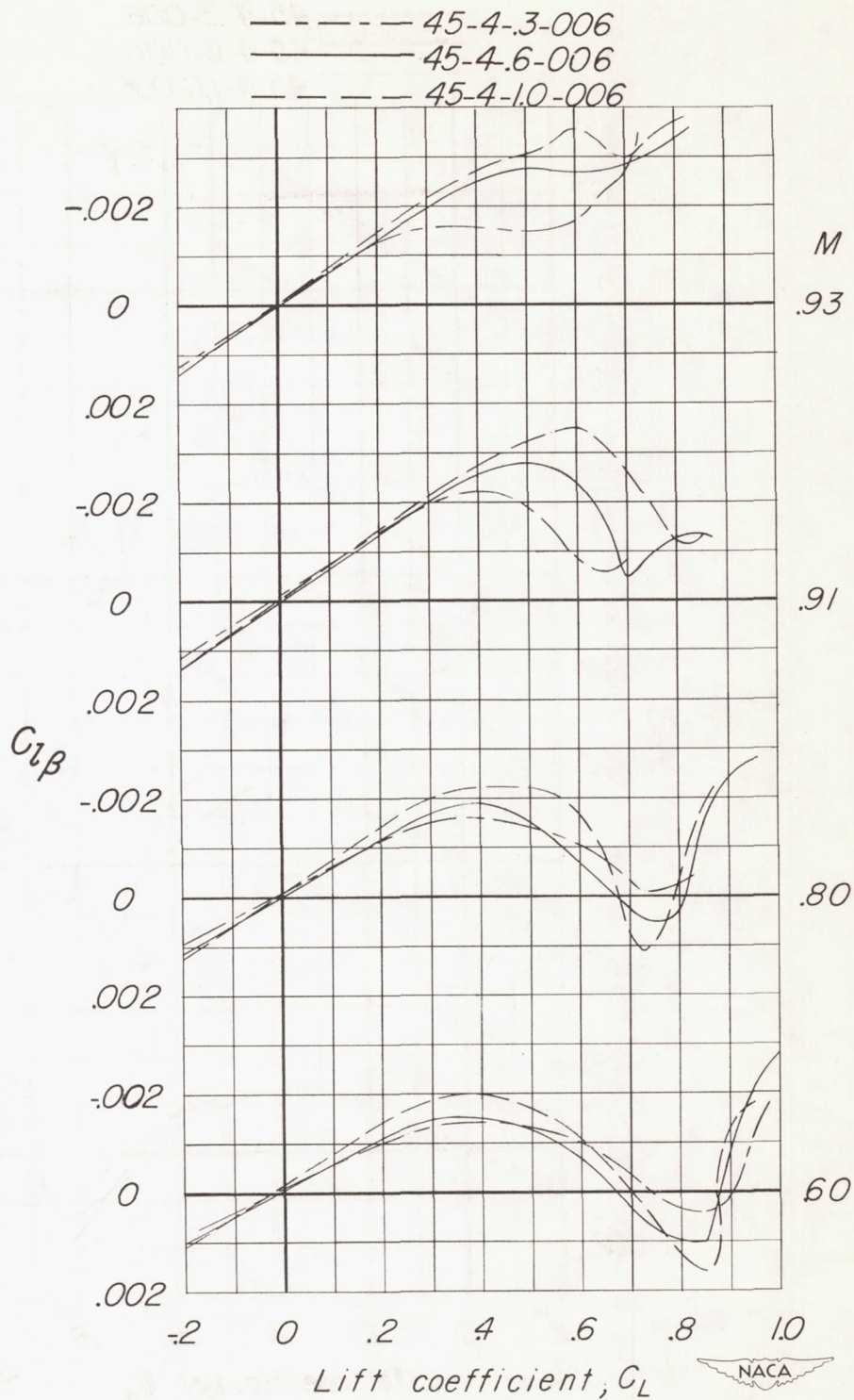
Figure 10.- Effects of taper ratio on the variation of C_{l_β} with lift coefficient for the wing-fuselage configurations at several Mach numbers. Data not corrected for aeroelastic distortion.
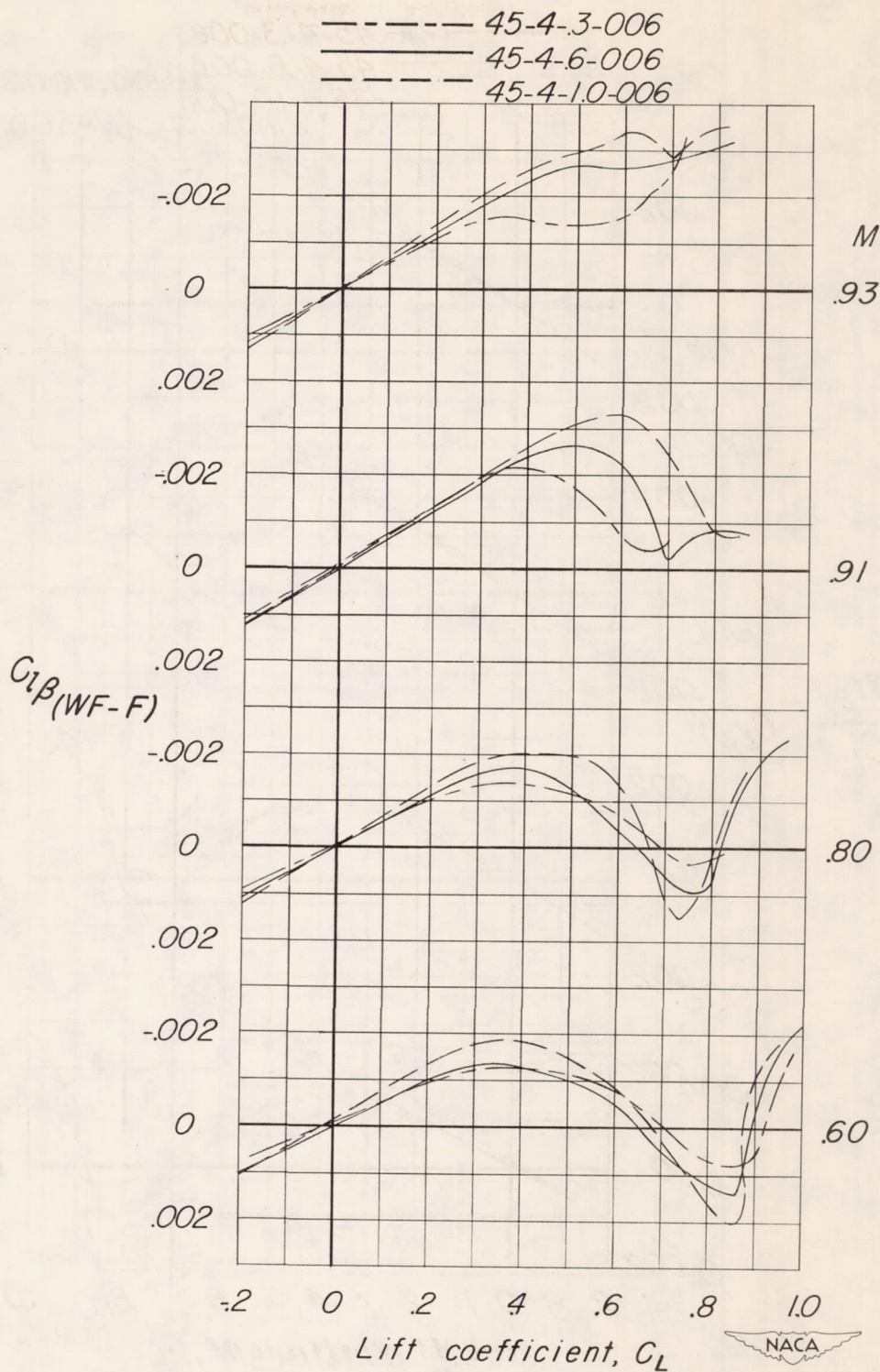
Figure 11.- Effects of taper ratio on the variation of wing-plus-wing-fuselage-interference values of C_{l_β} with lift coefficient at several Mach numbers. Data not corrected for aeroelastic distortion.
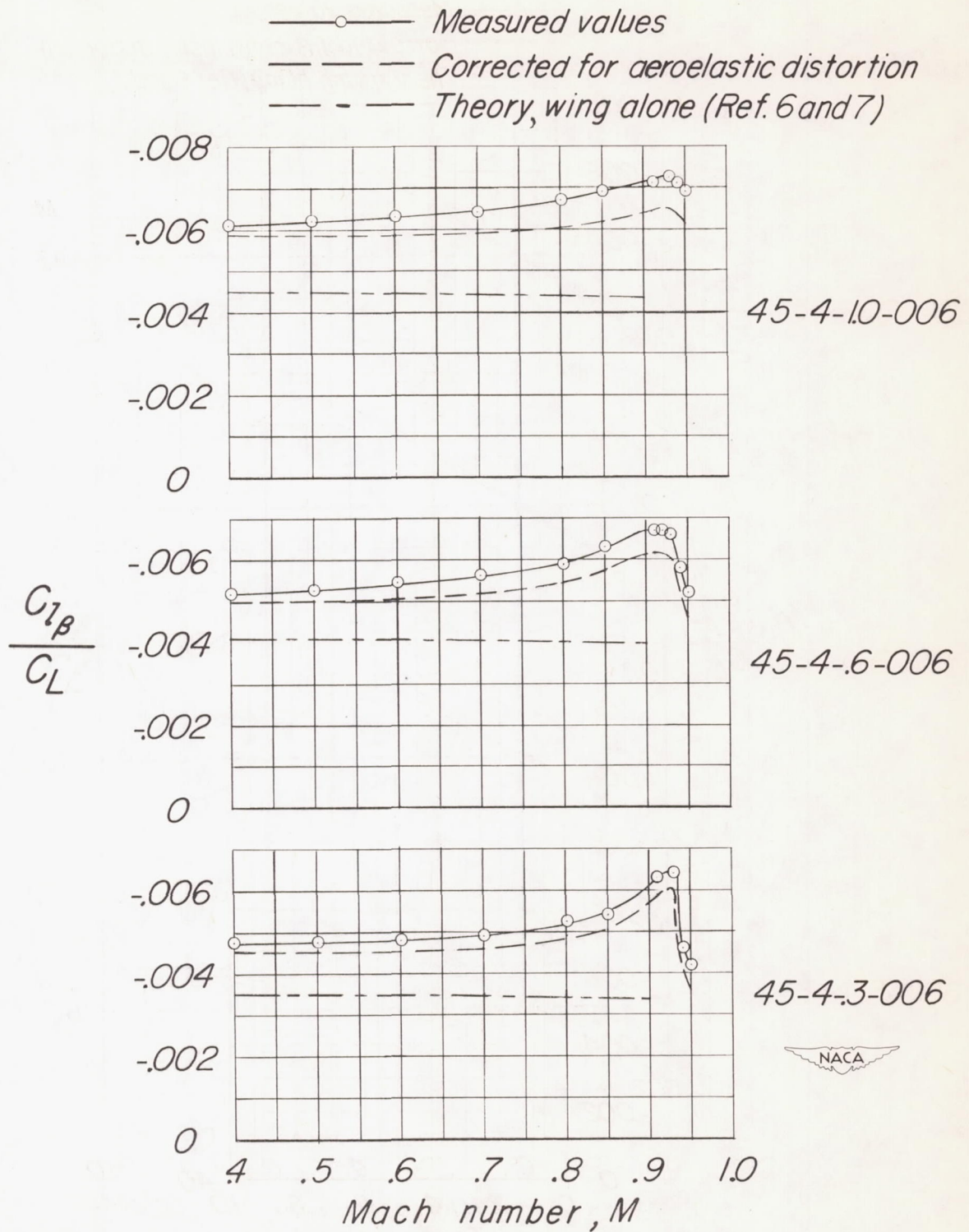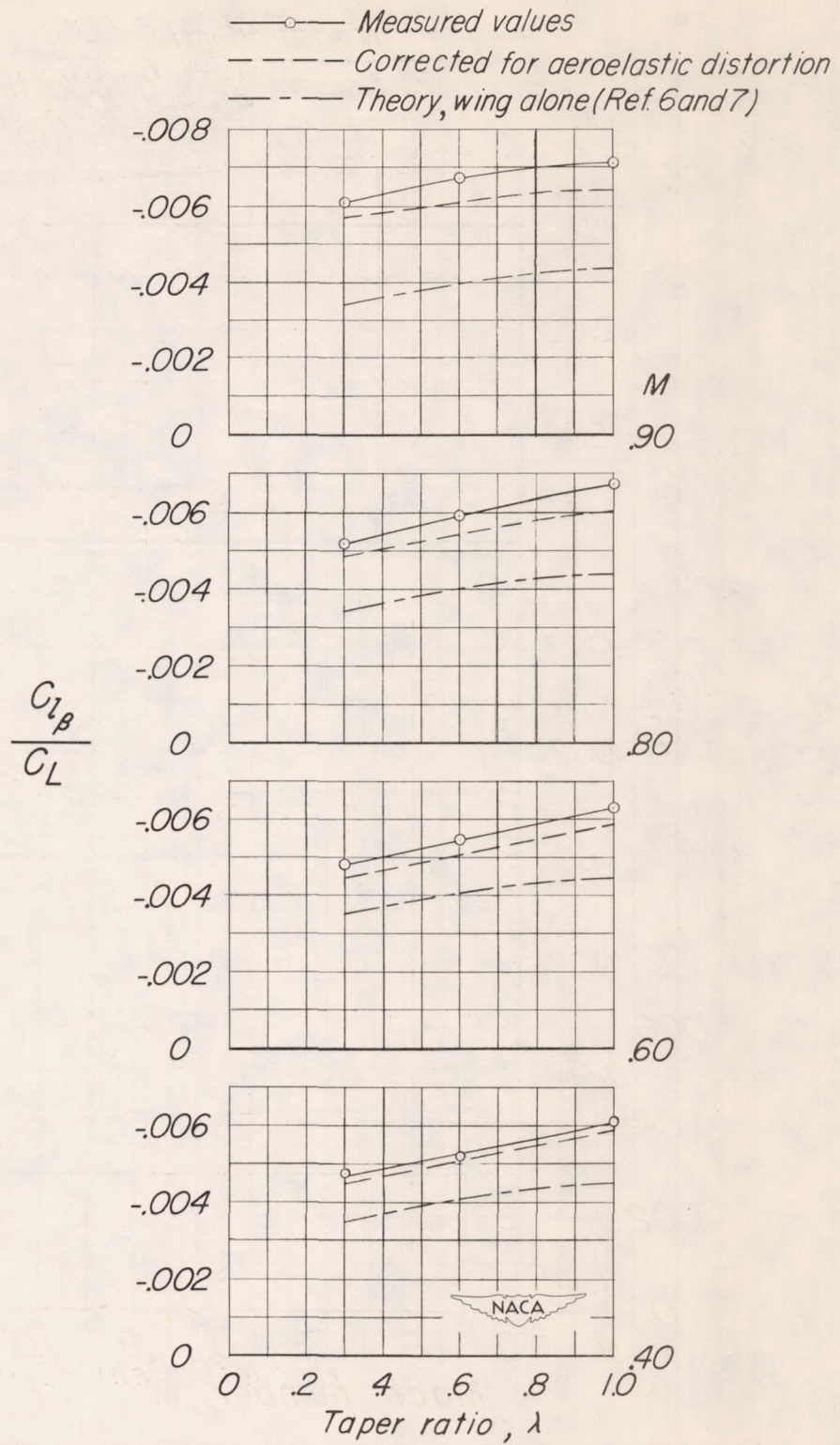
Figure 12.- Variation of C_{l_β}/C_L with Mach number.

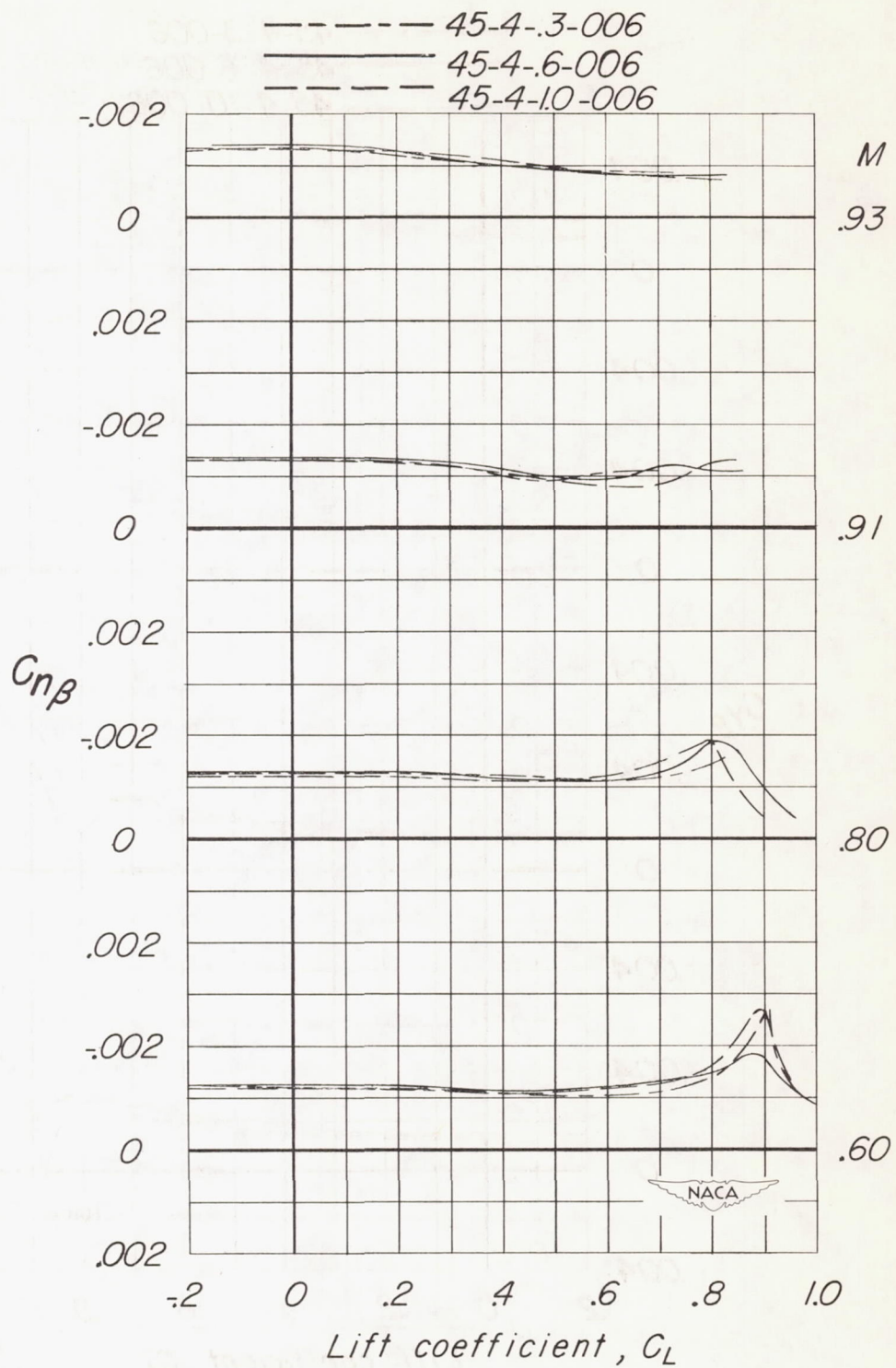Figure 13.- Variation of C_{l_β}/C_L with taper ratio.

Figure 14.- Effects of taper ratio on the variation of C_{n_β} with lift coefficient for the wing-fuselage configurations at several Mach numbers.
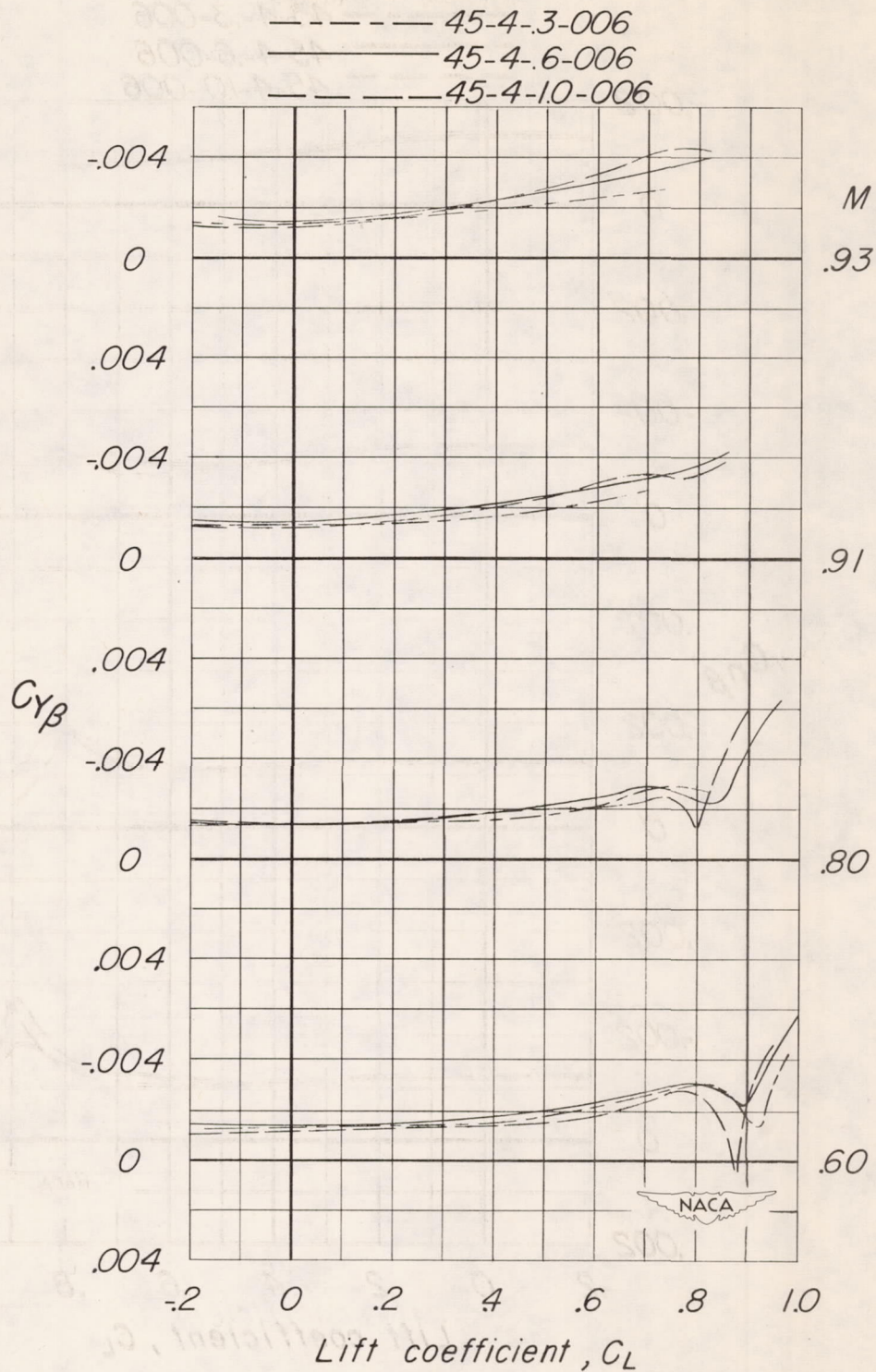
Figure 15.- Effects of taper ratio on the variation of C_{Y_β} with lift coefficient for the wing-fuselage configurations at several Mach numbers.
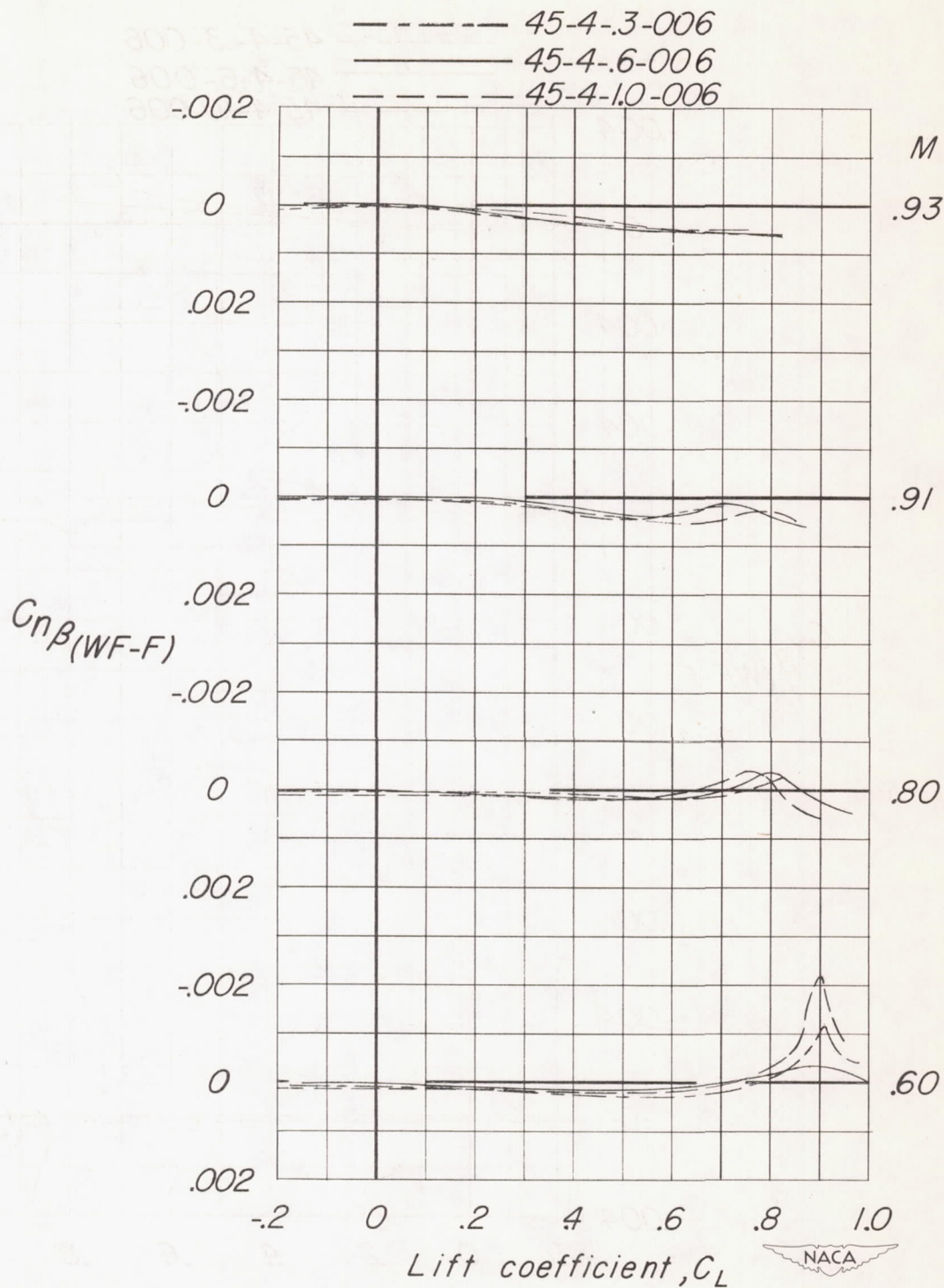
Figure 16.- Effects of taper ratio on the variation of wing-plus-wing-
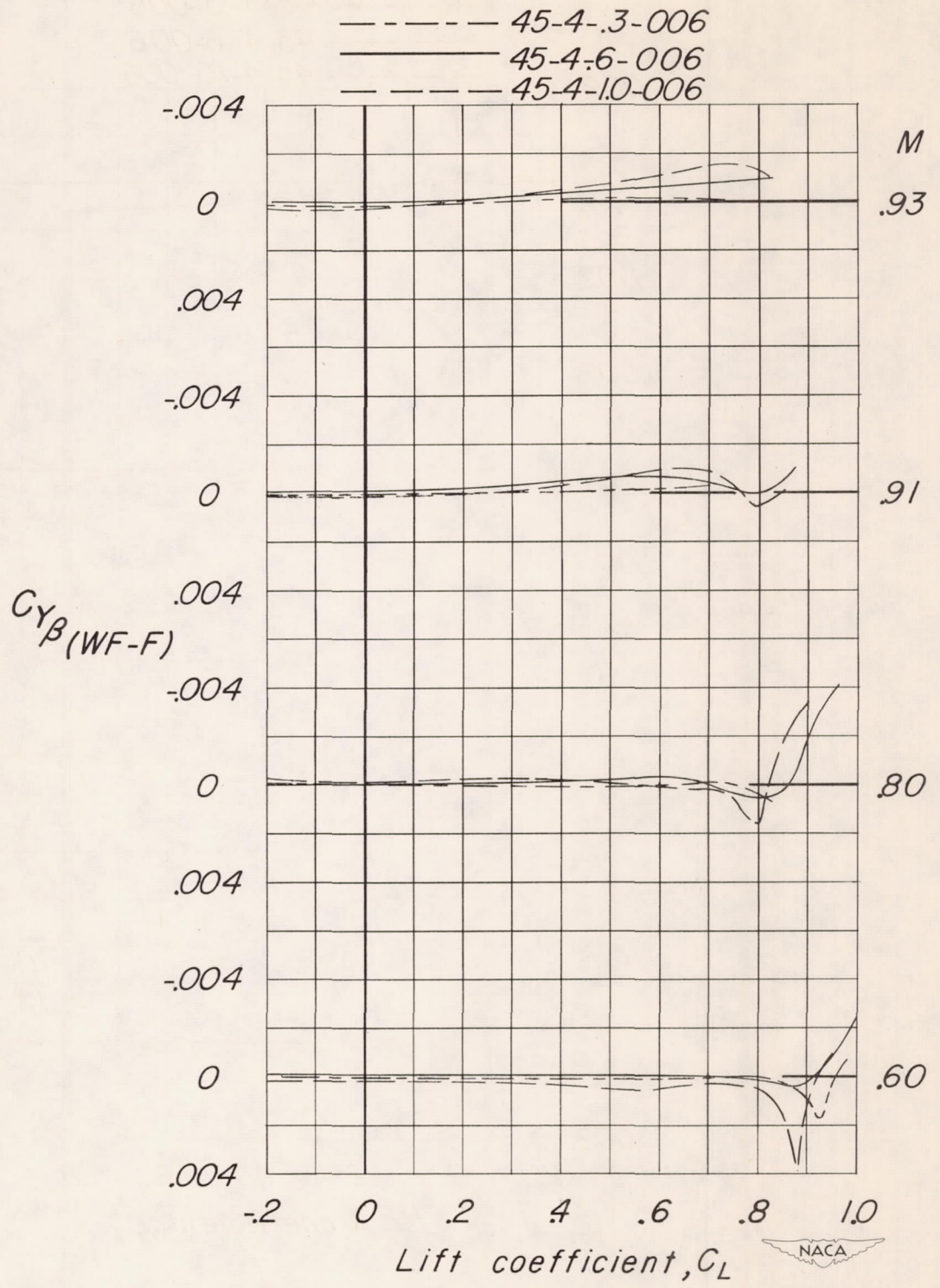fuselage-interference values of C_{n_β} with lift coefficient at several

Mach numbers.

Figure 17.- Effects of taper ratio on the variation of wing-plus-wing-
fuselage-interference values of C_{Y_β} with lift coefficient at several
Mach numbers.